

Thermodynamic properties and neutron diffraction studies of silver ferrite AgFeO_2

This article has been downloaded from IOPscience. Please scroll down to see the full text article.

2010 J. Phys.: Condens. Matter 22 016007

(<http://iopscience.iop.org/0953-8984/22/1/016007>)

View [the table of contents for this issue](#), or go to the [journal homepage](#) for more

Download details:

IP Address: 129.252.86.83

The article was downloaded on 30/05/2010 at 06:29

Please note that [terms and conditions apply](#).

Thermodynamic properties and neutron diffraction studies of silver ferrite AgFeO_2

A Vasiliev¹, O Volkova¹, I Presniakov¹, A Baranov^{1,2}, G Demazeau²,
J-M Broto³, M Millot³, N Leps⁴, R Klingeler⁴, B Büchner⁴,
M B Stone⁵ and A Zheludev⁶

¹ Moscow State University, 119991 Moscow, Russia

² Institut de Chimie de la Matière Condensée de Bordeaux, CNRS, Université de Bordeaux,
86 Avenue Dr Schweitzer, 33608 Pessac, France

³ Laboratoire National des Champs Magnétiques Intenses (LNCMI)—CNRS UPR 3228,
Université de Toulouse, 143 Avenue de Rangueil, 31400 Toulouse, France

⁴ Leibniz Institute for Solid State and Materials Research, IFW Dresden, 01171 Dresden,
Germany

⁵ Oak Ridge National Laboratory, PO Box 2008, Oak Ridge, TN 37831, USA

⁶ Laboratory for Neutron Scattering, Swiss Federal Institute of Technology Zurich and Paul
Scherrer Institute, 5232 Villigen, Switzerland

Received 14 September 2009, in final form 27 October 2009

Published 3 December 2009

Online at stacks.iop.org/JPhysCM/22/016007

Abstract

We present thermodynamic and neutron scattering data on silver ferrite AgFeO_2 . The data imply that strong magnetic frustration $\Theta/T_N \sim 10$ and magnetic ordering arise via two successive phase transitions at $T_2 = 7$ K and $T_1 = 16$ K. At $T < T_2$, two metamagnetic phase transitions at $B_1 \sim 14$ T and $B_2 \sim 30$ T can be identified through the change of slope in the magnetization curve measured up to 53 T. These transitions roughly correspond to an eighth and a quarter of the saturation magnetizations. Unlike for the ‘classical’ delafossite CuFeO_2 , the wavevector of the magnetic structure is independent of temperature both at $T < T_2$ and at $T_2 < T < T_1$.

(Some figures in this article are in colour only in the electronic version)

1. Introduction

Owing to their numerous applications as catalysts and batteries, luminescent materials and transparent conductors the delafossite-type oxides ABO_2 have been studied very intensely. The specific fields of use for these compounds are determined by their chemical composition. The A-site cations with completely filled d orbitals, $\text{Cu}^+(3d^{10})$ and $\text{Ag}^+(4d^{10})$, are most appropriate for applications in optics, while the B-site cations with partially filled d orbitals are important elements for the development of batteries and catalysts (see, e.g., the review [1] and references therein). Since either one or two cationic positions in the delafossites could be occupied by the transition metal ions, the issue of magnetism in these quasi-two-dimensional compounds is also important, so that another powerful impetus to their study is the physics of strongly frustrated magnetic systems [2].

The most studied member in the ABO_2 family is the ‘delafossite’ itself, i.e. CuFeO_2 (see recent papers [3–5] and references therein). In this compound, the Cu^{1+} ions do

not exhibit a magnetic moment, while the Fe^{3+} ($3d^5$) ions with half-filled 3d orbitals possess a spin moment $S = 5/2$ and no orbital moment. This fact suggests their Heisenberg-type character. The structure and the orbital configuration imply magnetic interactions of antiferromagnetic nature which frustration is expected to be removed by the formation of a non-collinear 120° magnetic structures within the triangular FeO_6 layers. These structures were found indeed in chromium-based delafossites LiCrO_2 [6] and CuCrO_2 [7].

It turned out, however, that the ‘classical’ delafossite CuFeO_2 exhibits an Ising-type character which is quite unexpected for the Fe^{3+} ions [8, 9]. The neutron scattering studies present evidence that its ground state is a collinear commensurate 4-sublattice ($\uparrow\uparrow\downarrow\downarrow$) structure with wavevector $(1/4, 1/4, 3/2)$. Upon heating, the system transforms into a sinusoidal amplitude modulated phase at $T_2 = 11$ K. In this phase, the four sublattice magnetic structure is replaced by an incommensurate phase, in which the magnetic Bragg reflections occur at positions $(q, q, (6m+3)/2)$, where m is an integer and the value of q is temperature dependent and ranges

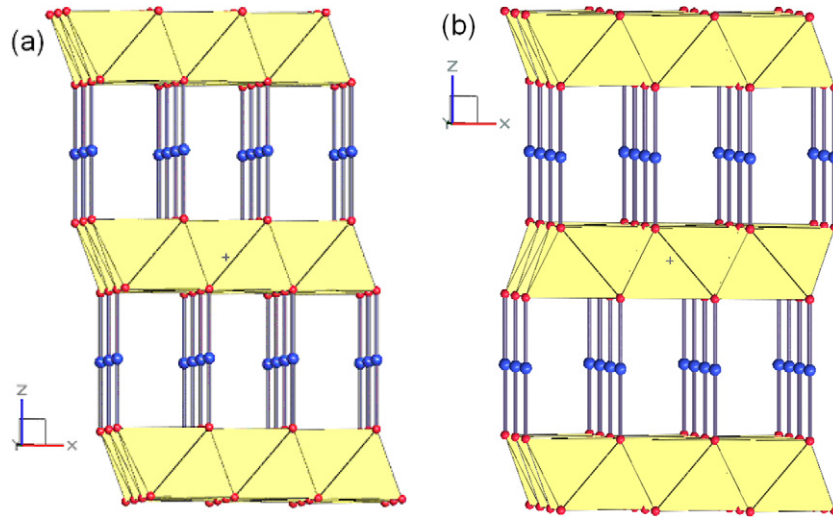


Figure 1. The polyhedral representation of the crystal structures of 3R (a) and 2H (b) polytypes of AgFeO_2 . Yellow octahedra are oxygen (red (smaller) spheres) coordinated Fe sites. Blue (larger) spheres are Ag sites.

Table 1. Crystal lattice parameters of AgFeO_2 and CuFeO_2 .

Compound	Crystal group	a (Å)	c (Å)	Reference
AgFeO_2 -2H	$P6_3/mmc$	3.0390	12.395	[19]
AgFeO_2 -3R	$R\bar{3}m$	3.0391	18.590	[18]
CuFeO_2	$R\bar{3}m$	3.0351	17.166	[20]

from 0.19 to 0.225. This collinear incommensurate phase transforms into a paramagnetic phase at $T_1 = 14$ K [10, 11]. The magnetic structure of CuFeO_2 is quite sensitive to external magnetic fields. A succession of metamagnetic phase transitions has been observed in a field-oriented powder. Monte Carlo simulations suggest that the successive critical magnetic fields correspond to transitions between various stable magnetic configurations [12]. The importance of magnetoelastic coupling in CuFeO_2 was revealed recently in synchrotron x-ray diffraction [13–15] and ultrasonic velocity measurements under external magnetic field [16, 17].

In the vast family of delafossites ABO_2 , one of the least studied members is the silver ferrite AgFeO_2 . To our knowledge, the available information on its properties is limited to the structural data on the two polytypes, i.e. rhombohedral 3R (space group $R\bar{3}m$) [18] and hexagonal 2H (space group $P6_3/mmc$) [19], crystal structures. The silver ferrite consists of alternate A layers of two-dimensional close-packed silver Ag^+ ($4d^{10}$) ions in the dumbbell O– Ag^+ –O coordination and B layers of slightly distorted edge-sharing (Fe^{3+}O_6) octahedra. The 3R and 2H polytypes differ by the stacking variants, as shown in figure 1. The crystal structure parameters of the 3R and 2H polytypes of AgFeO_2 [18, 19] along with those of CuFeO_2 [20] are given in table 1. Having the same closed shell electronic configuration of the A layer as CuFeO_2 , the silver ferrite is a semiconductor, which was proven experimentally [20], but electronic band structure calculations are still debated [21–23].

Despite the fact that silver ferrite AgFeO_2 belongs to the already known and well studied delafossites the investigation

of every new member in this family may shed new light on the basic properties of these heavily frustrated magnets. The goal of our study was to provide characterization of the local structure and the magnetic behavior of the AgFeO_2 ferrite through neutron diffraction techniques and measurements of its thermodynamic properties in the range 1.8–300 K and magnetic fields up to 53 T.

2. Experimental details

Since the binary oxide of silver Ag_2O decomposes at about 300°C , a single step solid-state synthesis of AgFeO_2 in open air is impossible. This difficulty can be overcome using a low temperature or closed reaction system. In the present study, a mixture of Ag_2O and Fe_2O_3 in equal ratio was placed into a Pt container and fired in an oxygen atmosphere at 700°C for 24 h at 0.15 MPa in a high pressure chamber.

The powder x-ray diffraction pattern of AgFeO_2 , collected with $\text{Cu K}\alpha$ radiation, is shown in figure 2. It indicates that the sample consists primarily of the 3R polytype, with a small amount of admixed 2H polytype. The x-ray pattern obtained is very similar to that of AgFeO_2 prepared by means of hydrothermal synthesis [1]. The magnetic susceptibility χ was measured at $B = 0.1$ T by means of a Quantum Design MPMS SQUID magnetometer. The measurements of magnetization M up to 53 T were performed in pulsed magnetic field. The specific heat C was studied in a Quantum Design PPMS in magnetic field up to 9 T.

The neutron diffraction measurements were performed using the HB1A fixed incident energy (14.62 meV, $\lambda = 2.3567$ Å) triple axis spectrometer located at Oak Ridge National Laboratory's High Flux Isotope Reactor. The sample consisted of approximately 0.8 g of AgFeO_2 powder loaded into an aluminum can with helium exchange gas. Measurements in the range 1.8–30 K were made with scanning wavevector transfer, Q , in 2-axis mode of the instrument with the analyzer turned orthogonal to the scattered beam.

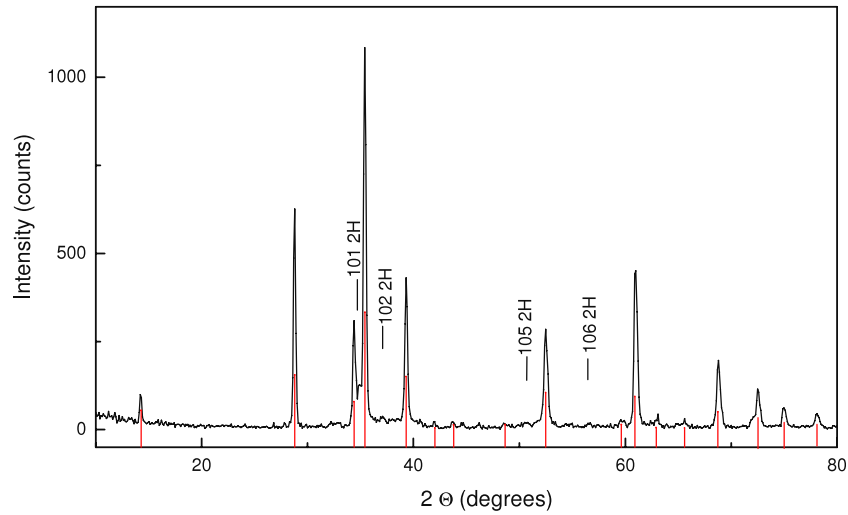


Figure 2. X-ray diffraction pattern of the AgFeO_2 powder sample consisting primarily of the 3R polytype, with a small amount of admixed 2H polytype. Red vertical lines correspond to indexed peaks of the 3R polytype based upon the structure described in [18]. Black vertical markers and text correspond to peak positions and indices of the 2H polytype based upon the structure described in [19].

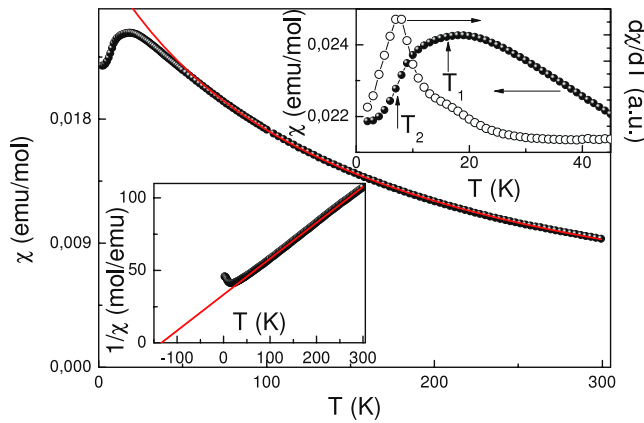


Figure 3. Temperature dependent magnetic susceptibility of AgFeO_2 . Measurements were made in an applied field of $B = 0.1$ T. The lower inset represents an inverse magnetic susceptibility, while the upper inset enlarges the low temperature region. The solid lines in the main panel and in the lower inset are the Curie–Weiss law. The positions of arrows in the upper inset correspond to anomalies in the specific heat of AgFeO_2 at $T_2 = 7$ K and $T_1 = 16$ K.

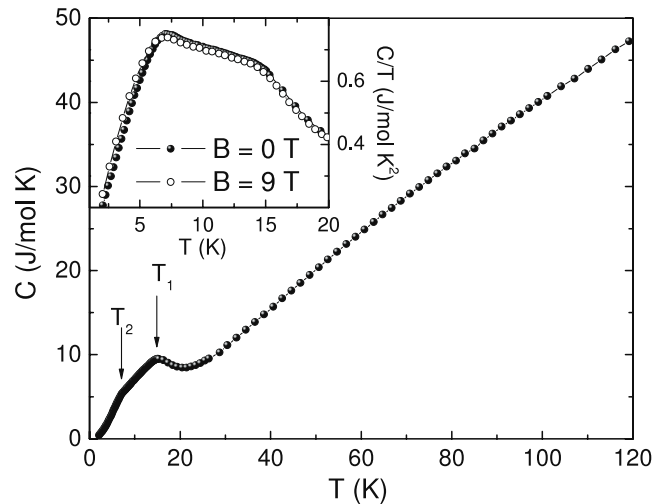


Figure 4. The temperature dependence of the specific heat of AgFeO_2 . The inset represents an enlarged low temperature region plotting C/T with curves taken at 0 and 9 T magnetic fields. The arrows indicate the successive magnetic phase transitions at $T_2 = 7$ K and $T_1 = 16$ K.

3. Results

The temperature dependence of the magnetic susceptibility $\chi(T)$ of AgFeO_2 is shown in figure 3. As follows from the lower inset to figure 3, in a wide temperature range, $70 \text{ K} < T < 300 \text{ K}$, it obeys the Curie–Weiss law with a negative Weiss temperature $\Theta = -140 \text{ K}$ and an effective magnetic moment $\mu_{\text{eff}} = 5.77 \mu_B$. This value is slightly lower than the value expected for Fe^{3+} ions with spin-only moments $S = 5/2$, $\mu_{\text{eff}} = 5.92 \mu_B$. At low temperatures, the magnetic susceptibility drops for about 10% revealing an irregular behavior in the range 2–20 K, as shown in the upper inset to figure 3.

In principle, one might speculate that the broad maximum in $\chi(T)$ dependence is a manifestation of

reduced dimensionality and correlation effects in magnetically frustrated layers of FeO_6 octahedra. The specific heat C data, shown in figure 4, indicate, however, that there are clear specific heat anomalies associated with phase transitions at $T_2 = 7 \text{ K}$ and $T_1 = 16 \text{ K}$. This behavior is highlighted by the C/T data in the inset of figure 4, which also shows that an external magnetic field of 9 T has only a negligible effect on the entropy changes.

At $T < T_2$, the results of pulsed magnetic field measurements, shown in figure 5, indicate two metamagnetic transitions at $B_1 \sim 14 \text{ T}$ and $B_2 \sim 30 \text{ T}$ roughly corresponding to 1/8 and 1/4 of saturation magnetization. The anomalies in the magnetization curve are associated with a small hysteresis when measuring as a function of increasing and decreasing

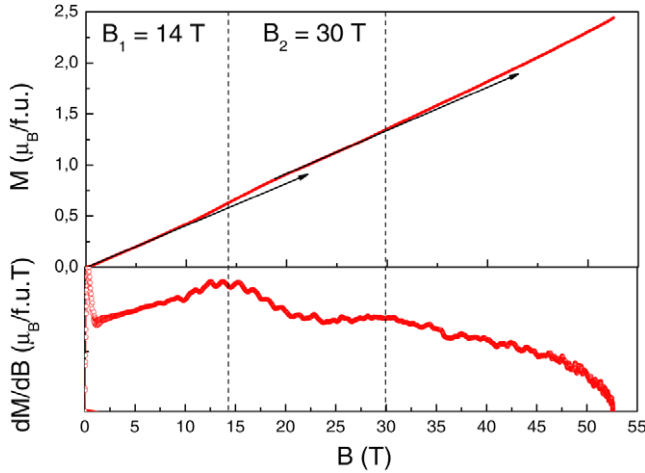


Figure 5. The magnetization of AgFeO_2 measured in pulsed magnetic field at 2 K. Black arrows are guides for an eye. The values of critical magnetic field B_1 and B_2 were obtained from the broad maxima in the derivative dM/dB for increasing magnetic fields.

magnetic field. This feature hence implies a first order nature of these metamagnetic phase transitions associated evidently with transformations in the magnetic subsystem of AgFeO_2 . Experimentally, the derivative of the magnetic flux by the induced voltage in compensated pick-up coils was measured, as shown in the lower panel of figure 5. From this signal up to 53 T and the measurements of the reference signal without sample within the pick-up coils, the magnetization curve $M(B)$ was integrated.

The neutron diffraction spectra of AgFeO_2 were measured in the range 1.8–30 K, the results of measurement at 30 K are shown in figure 6. The nuclear diffraction peaks are consistent with those calculated based upon the hexagonal lattice constants of [18] with space group $R\bar{3}m$. Figure 7 shows the temperature dependence of scattering intensity versus Q characterizing diffraction measurements of AgFeO_2 for a series of temperatures focusing on smaller wavevectors. Additional diffraction peaks at small wavevectors appear as the temperature is reduced. This is consistent with these reflections being magnetic in origin. Additional diffraction peaks are measured in the vicinity of $0.75\text{--}1 \text{ \AA}^{-1}$ and in the vicinity of 1.75 \AA^{-1} . There appears to be two magnetic transitions: one at about $T_2 = 7 \text{ K}$ and another at about $T_1 = 16 \text{ K}$. We do not observe any significant shift in the position of these peaks as a function of temperature.

We have calculated the wavevectors of potential magnetic Bragg peaks for hexagonal symmetry of the undistorted $R\bar{3}m$ space group for $h = \frac{m}{\delta}$, $k = \frac{n}{\delta}$, and $l = \frac{p}{\varepsilon}$, where m , n , and p are integers and combinations of δ and ε being 2, 3 or 4. The lowest wavevector magnetic peak at $Q = 0.812(6) \text{ \AA}^{-1}$ for $T < T_2$ indexes well to $(1/3 \ 0 \ 1/2)$ or an equivalent hexagonal wavevector ($Q = 0.814 \text{ \AA}^{-1}$). The next clear magnetic wavevector at $Q = 0.953(2) \text{ \AA}^{-1}$ for $T_2 < T < T_1$ indexes well to $(2/3 \ 0 \ 2)$ or an equivalent hexagonal wavevector ($Q = 1.729 \text{ \AA}^{-1}$). Unfortunately, the small quantity of powder sample and the likelihood of many

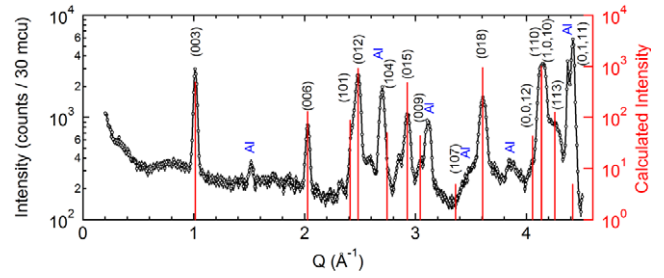


Figure 6. Scattering intensity versus Q for the $T = 30 \text{ K}$ measurement of AgFeO_2 . Data points are plotted as lines between open circles to illustrate measured points density. Error bars are shown and are typically smaller than the symbol size. Right axis is the calculated scattering intensity (logarithmic scale and arbitrary units) based upon the lattice parameters given in [18]. There are several very weak peaks which are indexed based upon them being due to the aluminum sample holder (Al) or cryostat. Count rates are in units of mcu (monitor count units) where the beam monitor was placed in the incident beam and $1 \text{ mcu} \sim 1 \text{ s}$.

overlapping peaks makes it difficult to index the magnetic peaks at larger wavevectors with certainty. We do not find an analogous peak at the $(1/4 \ 1/4 \ 3/2)$ wavevector as is observed in the CuFeO_2 delafossite. Based upon the indexed peaks at small wavevectors, it is likely that the ordered magnetic structures are 120° spirals with different basis vectors in the two portions of the magnetic phase diagram. Upon lowering temperature, the additional peaks associated with the formation of long-range magnetic order appear at T_1 and are seen down to T_2 . At T_2 these peaks disappear, but new ones appear at different wavevectors. In a narrow range around T_2 the peaks corresponding to two different magnetic phases coexist.

4. Discussion

In general, the behavior of silver ferrite resembles strongly that of ‘classical’ delafossite CuFeO_2 . Similar to the latter compound, the AgFeO_2 exhibits two phase transitions at low temperatures, corresponding to the formation of different magnetic structures below T_1 and in the range $T_2 < T < T_1$. Unlike the situation in CuFeO_2 the wavevector of the magnetic structure in the range $T_2 < T < T_1$ appears to be temperature independent. The specific heat data show that a moderate magnetic field has no significant effect on the entropy changes. It seems that the exchange interaction parameters in AgFeO_2 exceed the corresponding values in CuFeO_2 . The Weiss temperature $\Theta \sim -140 \text{ K}$ in the former compound is to be compared with the Weiss temperature $\Theta \sim -70 \text{ K}$ in the latter compound [9]. The silver ferrite appears to be more frustrated since the ratio of Weiss temperature Θ and magnetic ordering temperature T_2 in AgFeO_2 is about 10, while it is about 5 in CuFeO_2 . This change in the energy scale is reflected in a higher value of the first metamagnetic transition field in silver ferrite, i.e. $B_1 = 14 \text{ T}$, as compared with that in copper ferrite which amounts to 8 T [12].

To explain the apparent Ising-like character of the Fe^{3+} ions and the formation of the collinear magnetic structures in CuFeO_2 at low temperatures the presence of defect ions

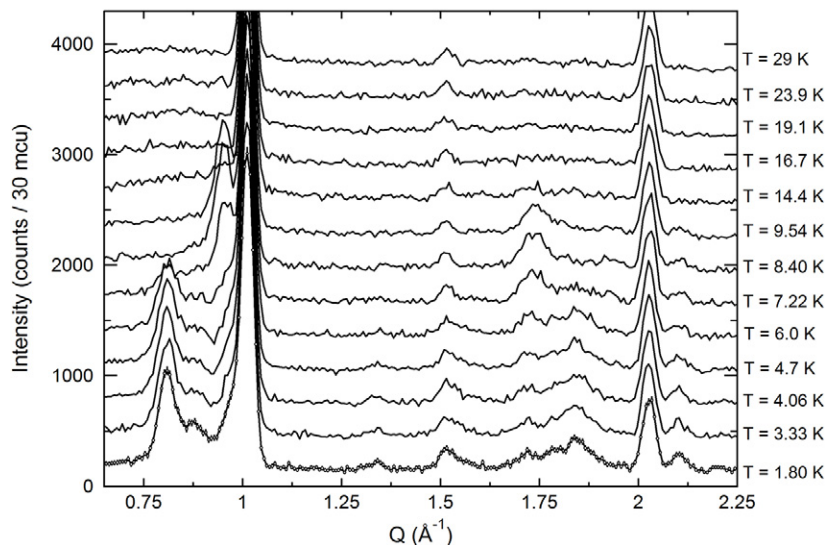


Figure 7. Scattering intensity versus Q for AgFeO_2 measured at different temperatures. Data are plotted over a narrow range of wavevector transfer to illustrate regions of magnetic scattering intensity. Data have been offset by multiples of 300 counts along the vertical axis for presentation. Individual point symbols with error bars are shown for the $T = 1.8$ K data.

Fe^{2+} and Cu^{2+} created by oxygen deficiency and oxygen excess, respectively, was postulated. The electron structure analysis [24] suggests that these defect ions generate uniaxial magnetic moments along the c -axis and hence induce the surrounding Fe^{3+} ions to orient their moments along the c -axis.

The applicability of the Ising model to the description of the triangular lattice in delafossites was questioned recently. A new model for understanding the magnetic properties of copper ferrite was proposed in [25] which differs significantly from the generally accepted two-dimensional Ising model. The analysis of magnetic susceptibility, magnetization and specific heat data on CuFeO_2 single crystals suggest a Heisenberg model with a relatively weak anisotropy to be proposed. The estimations for the main exchange interaction parameter J and the magnetocrystalline anisotropy D indicate that these two values differ by two orders of magnitude. It was suggested that besides the set of intralayer exchange interactions, the interlayer exchange interactions are crucial for the formation of the magnetic order in delafossites. Since the value of the critical field of the first metamagnetic phase transition in AgFeO_2 is of the same order of magnitude as the respective value in CuFeO_2 the analysis given for the latter compound could be applicable to the silver ferrite, too.

5. Conclusion

A study of the thermodynamic properties and neutron scattering characterization were performed on silver ferrite AgFeO_2 . It was found, that the magnetic ordering in this compound takes place via two successive phase transitions at $T_2 = 7$ K and $T_1 = 16$ K. Unlike the case of the ‘classical’ delafossite CuFeO_2 the wavevector of the magnetic structure in the range $T_2 < T < T_1$ is independent of temperature. At $T < T_2$, the changes of slope in the magnetization curve at 14 and 30 T evidence the metamagnetic phase transitions, roughly

corresponding to 1/8 and 1/4 of saturation magnetization. In general, the silver ferrite appears to be a more frustrated system with higher values of exchange interaction parameters as compared to the copper ferrite.

Acknowledgments

This work was supported by RFBR grants 07-02-00350, 07-02-92000, DFG grant 436 RUS and ISTC grant 3501 and EuroMagNet. A portion of this Research at Oak Ridge National Laboratory’s High Flux Isotope Reactor was sponsored by the Scientific User Facilities Division, Office of Basic Energy Sciences, US Department of Energy.

References

- [1] Sheets W C, Mugnier E, Barnabe A, Marks T J and Poepelmeier K R 2006 *Chem. Mater.* **18** 7
- [2] Moessner R and Ramirez A 2006 *Phys. Today* **59** 24
- [3] Ye F, Fernandez-Baca J A, Fishman R S, Ren Y, Kang H J, Qiu Y and Kimura T 2007 *Phys. Rev. Lett.* **99** 157201
- [4] Mitamura H, Mitsuda S, Kanetsuki S, Katori H A, Sakakibara T and Kindo K 2007 *J. Phys. Soc. Japan* **76** 094709
- [5] Terada N, Mitsuda S, Fujii T and Petitgrand D 2007 *J. Phys.: Condens. Matter* **19** 145241
- [6] Kadowaki H, Takei H and Motoya K 1995 *J. Phys.: Condens. Matter* **7** 6869
- [7] Kadowaki H, Kikuchi H and Ajiro Y 1990 *J. Phys.: Condens. Matter* **2** 4485
- [8] Mekata M, Yaguchi N, Takagi T, Sugino T, Mitsuda S, Yoshizawa H, Hosoito N and Shinjo T 1993 *J. Phys. Soc. Japan* **62** 4474
- [9] Takagi T and Mekata M 1995 *J. Phys. Soc. Japan* **64** 4609
- [10] Takeda K, Miyake K, Hitaka M, Kawae T, Yaguchi N and Mekata M 1994 *J. Phys. Soc. Japan* **63** 2017
- [11] Petrenko O A, Balakrishnan G, Lees M R, Paul D M and Hoser A 2000 *Phys. Rev. B* **62** 8983

- [12] Ajiro Y, Asano T, Takagi T, Mekata M, Aruga Katori H and Goto T 1994 *Physica B* **201** 71
- [13] Ye F, Ren Y, Huang Q, Fernandes-Baca J A, Dai P C, Lynn J W and Kimura T 2006 *Phys. Rev. B* **73** 220404
- [14] Terada N, Tanaka Y, Tabata Y, Katsumata K, Kikkawa A and Mitsuda S 2006 *J. Phys. Soc. Japan* **75** 113702
- [15] Terada N, Narumi Y, Sawai Y, Katsumata K, Staub U, Tanaka Y, Kikkawa A, Fukui T, Kindo K, Yamamoto T, Kanmuri R, Hagiwara M, Toyokawa H, Ishikawa T and Kitamura H 2007 *Phys. Rev. B* **75** 224411
- [16] Quirion G, Tagore M J, Plumer M L and Petrenko O A 2008 *Phys. Rev. B* **77** 094111
- [17] Quirion G, Plumer M L, Petrenko O A, Balakrishnan G and Proust C 2009 *Phys. Rev. B* **80** 064420
- [18] Prewitt C T, Shannon R D and Rogers D B 1971 *Inorg. Chem.* **10** 719
- [19] Okamoto S, Okamoto I and Ito T 1972 *Acta Crystallogr. B* **28** 1774
- [20] Rogers D B, Shannon R D, Prewitt C T and Gillson J L 1971 *Inorg. Chem.* **10** 723
- [21] Seshadri R, Felser C, Thieme K and Tremel W 1998 *Chem. Mater.* **10** 2189
- [22] Ong K P, Bai K, Blaha P and Wu P 2007 *Chem. Mater.* **19** 634
- [23] Ong K P, Bai K and Wu P 2008 *J. Alloys Compounds* **449** 366
- [24] Whangbo M-H, Dai D, Lee K-S and Kremer R K 2006 *Chem. Mater.* **18** 1268
- [25] Petrenko O A, Lees M R, Balakrishnan G, de Brion S and Chouteau G 2005 *J. Phys.: Condens. Matter* **17** 2741